PHYSICAL REVIEW B VOLUME 15, NUMBER 3 1 FEBRUARY 1977

Neutron scattering study of the spin dynamics and spin-wave form factor of chromium*

S. K. Sinha,† G. R. Kline, C. Stassis, and N. Chesser‡
Ames Laboratory-ERDA and Department of Physics, Iowa State University, Ames, Iowa 50011

N. Wakabayashi
Solid State Division, Oak Ridge National Laboratory,§ Oak Ridge, Tennessee 37830
(Received 7 June 1976)

The spin excitations in a single crystal of $Cr_{0.98}Mn_{0.02}$ have been studied by inelastic neutron scattering. High-resolution triple-axis spectrometer measurements have yielded a value of the spin-wave velocity at $T/T_N \simeq 0.5$ of $(1.30 \pm 0.15) \times 10^7$ cm/sec in good agreement with earlier measurements. The excitation strength drops extremely rapidly in the vicinity of T_N and decreases approximately linearly above T_N. The spin-wave form factor has been measured below and above T_N by measuring the spin-wave intensity at various superlattice points, and is found to agree to within experimental error with the static spin form factor. The implications of these results for the theory of itinerant electron antiferromagnetism are discussed.

I. INTRODUCTION

A considerable amount of experimental and theoretical effort has been directed toward an understanding of antiferromagnetism in chromium. It is by now well established that the spin-density wave (SDW) is associated with the conduction electrons, and that the generalized susceptibility function exhibits a peak at the incommensurate wave vector of the SDW.[1-5] While an application of the conventional theory of itinerant-electron antiferromagnetism gives a qualitative understanding of the experimental results, some discrepancies remain. The value of the measured spin-wave velocity in the ordered phase is lower by more than a factor of 2 than that predicted by the theory. The values of the exchange interaction obtained from the bulk spin susceptibility and the measured energy gap are inconsistent. Also, there is some question as to whether Hund's-rule type of interactions produce local-moment behavior in this system.

A variety of neutron scattering techniques have been used to investigate various aspects of the antiferromagnetism in chromium and chromium alloys: the spin-density form factor in the ordered state,[6] the induced-moment form factor in an applied magnetic field,[7] and the low-lying spin excitations in the ordered and paramagnetic phases.[8-11] In the present experiment, inelastic neutron scattering techniques have been used to measure the spin-wave velocity and the spin-wave form factor on a $Cr_{0.98}Mn_{0.02}$ alloy single crystal. This was chosen for reasons of experimental convenience, since in this system the SDW becomes commensurate, with twice the lattice periodicity.

There are discrepancies among the values of the spin-wave velocity obtained in earlier neutron scattering measurements. Sinha *et al.*[9] obtained a value $C = (1.29 \pm 0.26) \times 10^7$ cm/sec using the so-called "diffraction method," in which one measures the width of the diffuse scattering peak around a magnetic Bragg reflection. On the other hand, Als-Nielsen and Dietrich[8] and Als-Nielsen, Axe, and Shirane[10] obtained values of 0.69×10^7 cm/sec and $(1.6 \pm 0.16) \times 10^7$ cm/sec, respectively, by triple-axis measurements. In these experiments the spin-wave velocity was obtained by fitting to the width of an unresolved peak centered around a magnetic-reciprocal-lattice point (in a constant-energy-transfer scan) and unfolding the resolution width. Unfortunately, the resolution is usually the dominant contribution to the width leading to sizeable uncertainties in the values of the spin-wave velocity.

Since the $\vec{q}$-space resolution (in directions perpendicular to as well as in the scattering plane) is the limiting factor in resolving the spin-wave peaks around the magnetic-reciprocal-lattice point, it was decided to repeat the triple-axis measurement at room temperature with good vertical as well as horizontal collimation. At high temperatures, close to the Néel point, the softening of the spin-wave velocity permits more relaxed collimation. However, the greater damping effects produce additional complications in the analysis. The present measurements have been performed on the HB-3 triple-axis spectrometer at the HFIR reactor at Oak Ridge National Laboratory, and they are discussed in Sec. II of the present paper.

Since chromium is an itinerant-electron system, it is of considerable interest to study the spatial distribution of the magnetization associated with the spin fluctuations. This spatial distribution is determined by the *spin-wave* form factor, as opposed to the *static* form factor obtained from measurements of the intensities of Bragg reflections

in the ordered state. Such a spin-wave form factor has not been measured before for an itinerant-electron system. Physically, these two form factors may be thought of as representing the distribution of electronic spin density which takes part in spin fluctuations and the equilibrium spin density, respectively. For local-moment magnetic systems, the two form factors become identical, since all the spin density associated with an atom "flips" together in a spin excitation. However, for itinerant-electron magnetic systems, this need not be the case. A consideration of the theory for spin excitations in such systems[12-14] shows that the spin-wave form factor is given by the Q dependence of suitably averaged matrix elements between occupied and excited conduction-band states. If higher excited-state matrix elements contribute appreciably, the spin density will undergo a deformation while "flipping" with a spin excitation. Paradoxically, the very reason which makes the spin-wave velocity so hard to measure in chromium-based antiferromagnets, namely, the high spin-wave velocity, makes it relatively easy to measure the spin-wave form factor, since it is sufficient to use poor resolution and obtain relative intensities of the (unresolved) peaks in a constant-E scan around the different magnetic-reciprocal-lattice points. These measurements were performed on a triple-axis spectrometer at the Ames Laboratory Research Reactor. Section III describes the spin-wave form factor measurements and those of the temperature dependence of the spin-wave intensity. Finally, in Sec. IV we discuss the implications of these measurements for our understanding of itinerant-electron antiferromagnetism.

II. SPIN-WAVE VELOCITY DETERMINATION

Figure 1 illustrates schematically the measurement of the spin-wave velocity using a triple-axis spectrometer in the constant-E mode of operation. This figure shows the projection on the ω-q_x plane of a cone in four dimensions representing the ω-vs-$\vec{q}$ linear dispersion surface, which is intersected by the four-dimensional resolution ellipsoid. Because of the large spin-wave velocity, the cone semiangle is very small and the peaks obtained from the above intersection are not resolved. An attempt was made to resolve these peaks by using the HB-3 triple-axis spectrometer at the HFIR reactor and fairly tight resolution. The monochromator and analyzer were beryllium crystals set for reflection by the (103) and (002) planes, respectively. The horizontal collimation was 20 min of arc before and after the sample, 1.2° before the monochromator, and 5° after the analyzer. The vertical collimation was 24 min of arc before the sample, 48 min after the sample, 1.5° before the monochromator and 5° after the analyzer. The mosaic spreads (full width at half maximum) of the monochromator and analyzer were 0.35° and 0.4°, respectively. The mosaic spread of the crystal was found to be negligible. The measurements were performed at room temperature.

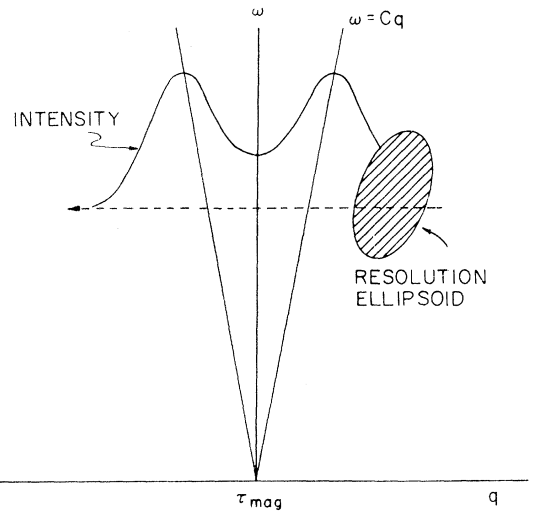

FIG. 1. Schematic illustration of how spin-wave peaks are obtained around magnetic reciprocal lattice points with constant-energy scans.

Figure 2 shows the data obtained in two constant-E scans (done in a direction transverse to [001]) around the (001) magnetic reflection with incident energies of 39.3 and 79.8 meV and with energy loss of 26.9 and 38.5 meV, respectively. The curves on Fig. 2 represent theoretical peak shapes calculated by folding the resolution functions of the spectrometer with delta functions on the spin-wave dispersion surface and assuming various values of the spin-wave velocity. No damping effects were allowed for, since these are believed to be small at room temperature. From these curves one may see that we may place the spin-wave velocity at $C = (1.30 \pm 0.15) \times 10^7$ cm/sec. The theoretical curve corresponding to this value of the spin-wave velocity is in good agreement with the experimental data (except for two points, at a reduced wave vector of 0.03 of the scan with incident energy of 39.29 meV, which, we believe, are contaminated by spurious effects). The spin-wave velocity obtained in the present experiment is in excellent agreement with the earlier measurements using the diffraction method,[9] and about 20% lower than the value measured for $T/T_N \simeq 0.5$ by Als-Nielsen *et al.*[10] which was, however, for a $Cr_{0.95}Mn_{0.05}$ alloy crystal.

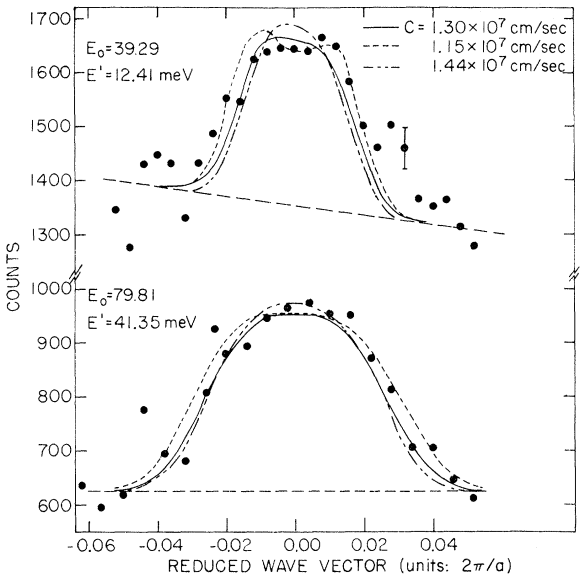

FIG. 2. Experimental points obtained by performing contant-E scans around the (1, 0, 0) magnetic reciprocal lattice vector. In this figure, E_0 and E' denote the incident and final neutron energies respectively. The theoretical curves are obtained by folding the instrumental resolution function with delta functions on the spin-wave dispersion cone assuming the indicated values of the spin-wave velocity C.

III. MEASUREMENT OF THE SPIN-WAVE FORM FACTOR

The spin-wave neutron scattering cross section is given by

$$\frac{d^2\sigma}{d\Omega d\omega} = \frac{2}{3}\left(\frac{\gamma r_0}{g\mu_B}\right)^2 \frac{k'}{k}\frac{e^{\beta\omega}}{e^{\beta\omega}-1}e^{-2W} \times\{2\mathrm{Im}[\chi_{+-}(\vec{Q},\vec{Q},\omega)]+\mathrm{Im}[\chi_{zz}(\vec{Q},\vec{Q},\omega)]\}, \quad (1)$$

where γ is the neutron magnetic moment in nuclear magnetons, r_0 is the classical electron radius, $\vec{k}', \vec{k}$ are the scattered and incident neutron wave vectors, $\vec{Q}=\vec{k}-\vec{k}'$, ω is the neutron energy loss, $\beta = 1/kT$, e^{-2W} is the Debye-Waller factor, and χ_{+-} and χ_{zz} are, respectively, the transverse and longitudinal components of the diagonal part of the generalized susceptibility function. In Eq. (1), we have used the fact that the domains with the ordered components of the spin along each of the cubic axes are equally populated. In the ordered phase, χ_{zz} is not believed to contribute to the inelastic scattering,[13-15] while in the paramagnetic case, by symmetry, $\chi_{zz}=\chi_{+-}$. Therefore, the cross section in Eq. (1) is always proportional to $\mathrm{Im}[\chi_{+-}(\vec{Q},\vec{Q},\omega)]$. We define the spin-wave form factor by writing

$$\chi_{+-}(\vec{Q},\vec{Q},\omega) = f^2(\vec{Q})\,\chi_{+-}(\vec{q},\omega), \quad (2)$$

where $\chi_{+-}(\vec{q},\omega)$ is assumed to depend only on $\vec{q}$, which is the scattering vector $\vec{Q}$ reduced to the first zone of the magnetic reciprocal lattice. This assumption is justified from the experimental results described below.

One may see from the above equations that the spin-wave form factor $f(\vec{Q})$ can be obtained by measurements, for $\vec{Q}$ at various magnetic superlattice points, of the integrated intensities in constant-E scans of the type shown in Fig. 1. However, corrections have to be made for the instrumental resolution, absorption in the sample, and the $\vec{Q}$ dependence of the Debye-Waller factor (unlike the case of intense Bragg reflections, extinction corrections for the very weak spin-wave intensities are negligibly small). The absorption correction was found to be negligible and the Debye-Waller factor was obtained from the calculations of Satya Pal.[16] The resolution function of the spectrometer was taken to be of the usual form[17,18]

$$R(\Delta\vec{Q},\Delta\omega) = R_0 \exp\left(-\frac{1}{2}\sum_{ij} M_{ij}\Delta x_i \Delta x_j\right), \quad (3)$$

where for $i = 1, 2, 3$, Δx_i denotes the Cartesian components of $\Delta\vec{Q}$, while Δx_4 stands for $\Delta\omega$. The parameters M_{ij} of the resolution function for the various experimental scans were obtained from the instrumental parameters which were estimated by fitting the theoretical expressions of Cooper and Nathans[17,18] to the measured resolution ellipsoids. The experiments were performed on two different triple-axis spectrometers at the Ames Laboratory Research Reactor. The resolution was intentionally chosen to be poor so that only one unresolved peak centered at $\vec{q}=0$ was seen in the constant-E scans.

Under the assumption that the dimensions of the dispersion surface for the ω at which the constant-E scan was made are very small compared with those of the resolution ellipsoid, it may be shown that the integrated intensity of the neutron group observed in a longitudinal scan through the superlattice point is given by

$$I(\vec{Q}) = C_0(k,k')\frac{e^{\beta\omega}}{e^{\beta\omega}-1}e^{-2W}f^2(\vec{Q}) \times\frac{\omega^2}{C^3\sin(2\theta_s)}[A'(M_{11}M_{44}-M_{14})]^{-1/2}. \quad (4)$$

For a transverse scan, M_{11}, M_{14} in Eq. (4) should be replaced by M_{22}, M_{24}, respectively. In Eq. (4), $C_0(k,k')$ is a constant which depends on fixed instrumental parameters, the incident flux, and on k, k' (all of which do not vary for scans around different superlattice points); $2\theta_S$ is the scatter-

ing angle at the sample and A' is a parameter defined in the paper of Cooper and Nathans.[17] The resolution parameters M_{ij} of course vary between superlattice points, and with ω. Thus, using Eq. (4), one may obtain relative values for $f(\vec{Q})$ at various magnetic reciprocal lattice points.

The measurements were performed at room temperature ($T/T_N = 0.51$). In order to ascertain whether the measurements were contaminated by multiple scattering, the integrated intensity ratios were measured for three different processes for which the neutron energy loss was 8.28, 12.42, and 16.56 meV, respectively. In addition, some integrated intensity ratios were measured using two different neutron incident energies (54.4 and 72.3 meV, respectively). The relative $f(\vec{Q})$'s obtained in this manner for the magnetic reciprocal lattice points [after correcting for all other factors in Eq. (4)] were found to agree within (10–15)%. In addition, the results for the ratio of integrated intensities obtained from transverse and longitudinal scans were consistent to within 10% with the predictions of the resolution function calculations. Thus, it seems extremely unlikely that the measurements are seriously contaminated by multiple scattering. In addition, the assumption of the ω independence of $f(\vec{Q})$ as written in Eq. (2) is seen to be valid. Figure 3 shows the measured spin-wave form factor normalized so that $f(\vec{Q})$ has the same value as the static form factor measured by Moon *et al.*[6] at the (001) superlattice reflection. Also shown is the $3d$-spin atomic form factor for Cr, as obtained from the calculations of Freeman and Watson,[19] which is essentially identical to the static form factor measured by Moon *et al.*[6] from the antiferromagnetic Bragg reflections of chromium. As may be seen, there is no significant difference between the spin-wave form factor and the static spin form factor.

By monitoring the intensity of the (001) magnetic Bragg reflection, the Néel temperature of the crystal used for these measurements was found to be $T_N = 577$ K. The form factor measurements were then repeated in the paramagnetic phase at $T = 647$ K, where well defined, although somewhat broadened, peaks were still observed at the magnetic reciprocal lattice points in the constant-E scans. These peaks correspond to the paramagnonlike excitations, which have been observed in earlier measurements.[8,9] The results for the paramagnon form factor at 647 K ($T/T_n = 1.12$) are also shown in Fig. 3 and, as can be seen, agree to within experimental precision with the room-temperature measurements.

In Fig. 4, we plot the temperature dependence of the integrated intensity of the peak obtained by

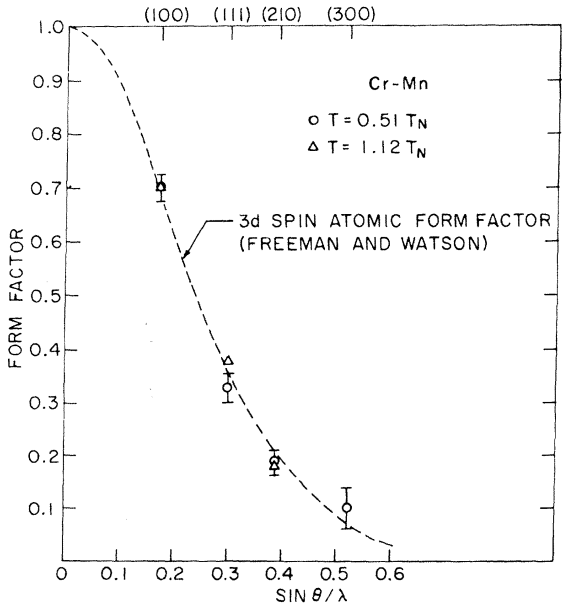

FIG. 3. Measured spin-wave form factors below and above T_N for $Cr_{0.98}Mn_{0.02}$ shown together with the Freeman-Watson $3d$ spin-atomic form factor. The experimental points are normalized so that the value at (0, 0, 1) is the same as the static form factor of Moon *et al.* (Ref. 6).

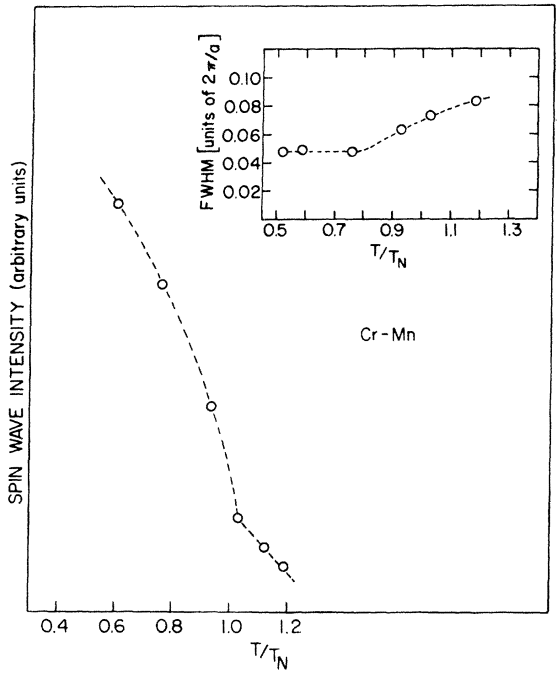

FIG. 4. Integrated intensity of the peak around (0, 0, 1) in a constant-E scan along [00ζ] is plotted against temperature. The full width at half maximum of the peak is plotted versus temperature in the insert.

a constant-E scan along $[00\zeta]$, around (0, 0, 1), for two different energy transfers, 8.28 and 16.56 meV. The integrated intensities plotted in this figure have been corrected for the temperature dependence of the population and Debye-Waller factors. Also plotted is the full width at half-maximum of the peak as a function of temperature. From the latter it appears that no dramatic softening or damping effects take place until $T \sim 0.75\, T_N$.

The rapid decrease of the intensity in the vicinity of the Néel temperature and the approximately linear decrease thereafter are particularly interesting. Unfortunately, it is impossible to correct this curve for instrumental resolution effects until one knows in detail how the scattering cross section actually varies with temperature in the vicinity of the Néel point. In the "undamped spin-wave" regime, Eq. (4) shows that a decrease of the spin-wave velocity with increasing temperature strongly affects the integrated intensity. The correction for instrumental resolution will cause the actual spin-wave intensity to decrease more rapidly than shown in Fig. 3 because of the factor $1/C^3$ in Eq. (4). The decrease of intensity with increasing temperature up to T_N is in fact reminiscent of the temperature dependence of the magnetic Bragg intensity itself, which goes as the square of the order parameter. It should be noted that this result is in complete contrast with the results of Tsunoda *et al.*[11] who find a much more gradual decrease of intensity. In Fe, on the other hand, Lynn[20] measured the temperature dependence of a 29-meV magnon intensity and found almost a linear decrease with temperature with no apparent discontinuity at T_c. Of course, near and above T_N, the undamped spin-wave picture undoubtedly breaks down and cannot be used to predict how the cross-section varies in this region. Above T_N, the theory of Liu[15] does, however, predict a logarithmic (and hence approximately linear near T_N) decrease of intensity with temperature.

IV. DISCUSSION

Our results indicate that the spin-wave dispersion in $Cr_{0.98}Mn_{0.02}$ is linear at small $\vec{q}$ with a slope of $(1.30 \pm 0.15) \times 10^7$ cm/sec. Attempts were made to look for an anisotropy gap at $\vec{q} = 0$ in the spin-wave spectrum but were unsuccessful. The conventional random-phase-approximation (RPA)-based theory of itinerant electron antiferromagnetism predicts a spin-wave velocity[15] of $(\frac{1}{3} v_a v_b)^{1/2}$ where v_a, v_b are the Fermi velocities of the two regions of the Fermi surface coupled by the electron-electron interaction. This has been estimated from band calculations[4] to be approximately 3×10^7 cm/sec. This large discrepancy may be taken to indicate a failure of the conventional RPA theory. However, recent work by Liu[21] appears to resolve the discrepancy. Liu treats the spin waves in terms of "quasispin" units on the atoms which behave very much like local moments, and yet preserve the itinerant nature of the electrons. This is basically an attempt to build in intra-atomic Hund's rule correlations which the conventional RPA theory leaves out. He finds the spin-wave energies renormalized by a factor of 0.3–0.42 which is of the right magnitude to agree with the experimental measurements. It would be very interesting to apply the theory to see whether it could account for the rapid decrease in spin-wave intensity in the vicinity of T_N, which is also reminiscent of local-moment-type behavior. The existence of inelastic neutron scattering around the magnetic reciprocal lattice sites above T_N could be interpreted either as "remnant spin waves" or as the paramagnon-type fluctuations also predicted by conventional theories of itinerant magnetism. It is to be noted that above T_N the latter predicts widths and a temperature dependence of the intensity which is *not* inconsistent with the experimental results.[15] However, NMR measurements in the region just above T_N[22] indicate local moment behavior in this region, and this has also been shown by Liu[21] to be consistent with his quasispin model. Another problem associated with the RPA itinerant model concerns the magnitude of the bulk static spin susceptibility. The exchange enhancement of the static spin susceptibility has been estimated by Stassis *et al.*[7] to be a factor of ~3, which would indicate a value of $N(E_F)U$ of ~0.67, where U is the strength of the electron-electron interaction and $N(E_F)$ is the density of states at the Fermi level for the electrons coupled by the interaction. Typical measurements of the antiferromagnetic gap,[23] however, yield values of $N(E_F)U$ of ~0.4.[15] Again, a quasilocal spin model could probably resolve this discrepancy.

We turn now to examine what the spin-wave form-factor measurements tell us about the quasispin and conventional RPA models of itinerant electron antiferromagnetism. The coincidence of the spin-wave form factor with the atomic $3d$ spin form factor could lead one to conclude that the system behaves like a set of completely localized rigid atomic spins, but this interpretation is too simplistic. The radial distribution of the d orbitals in the unit cell in chromium varies considerably across the width of the d band. The lower d states are primarily of t_{2g} bonding character and are relatively spatially extended, while the upper d states are primarily of e_g antibonding character and are much more contracted. How-

ever, the Fermi level lies close to the bottom of the valley in the density of states *between* the bonding and antibonding states, and it has been shown by Oh *et al.*[24] that the form factor associated with the states at the Fermi level of chromium is not too different from the free atom $3d$ form factor and is in reasonably good agreement with the spin part of the induced moment form factor measured by Stassis *et al.*,[7] and the static form factor in the ordered state as measured by Moon *et al.*[6] On the other hand, Gupta and Sinha[4] have calculated the diagonal part of the spin generalized susceptibility function $\chi(\vec{Q},\vec{Q})$ for chromium using the actual APW wave functions and energy levels for the first six bands. A similar calculation has been done by Windsor.[5] It is to be noted that this includes contributions from both intraband and interband transitions, with the latter dominating at larger $\vec{Q}$. If one naively assumes exchange enhancement effects to be the same for all bands, it may be shown that the $\vec{Q}$ dependence of $\chi(\vec{Q},\vec{Q})$ (for the small ω's of interest here), suitably normalized, yields the square of the spin-wave form factor. The $f(Q)$ obtained in this manner is shown in Fig. 5 where it is seen to be much more extended in $\vec{Q}$ space than the measured form factor. This is presumably due to the influence of the interband transitions, since the higher bands have more contracted wave functions. The implication is that if one wishes to use the conventional itinerant model of antiferromagnetism, one must

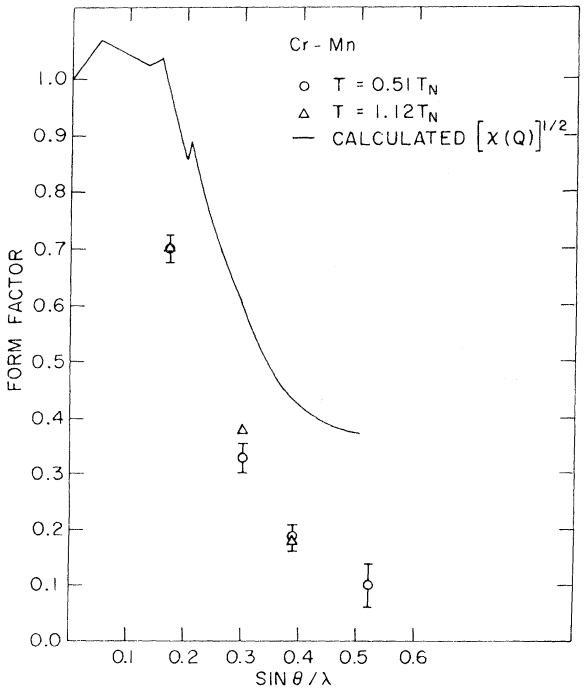

FIG. 5. Measured spin-wave form factors shown together with the function $[\chi(\vec{Q},\vec{Q})]^{1/2}$ (from Ref. 4).

perform a truly self-consistent multiband calculation,[13] and that in such a calculation the exchange enhancement of the intraband transitions at the Fermi level must dominate over the interband transitions. This is not unreasonable in view of the fact that both intra-atomic and interatomic exchange integrals are larger for transitions between t_{2g}-type orbitals than between t_{2g}- and e_g-type orbitals; and that the associated energy denominators are much smaller for intraband than interband transitions.

On the other hand, in the quasispin model, the spin-wave form factor would naturally be expected to be the same as the static form factor, except for "spin deformation" effects within the ion. Such deformation effects must be due to virtual transitions to excited states and are the analog of the interband transitions above. The experimental results indicate the absence of such deformation.

In conclusion, while the spin-wave form-factor measurements do not by themselves prove the existence of precessing quasispins in chromium, there seems to be various pieces of evidence indicating that the conventional RPA theories which start from the single-particle picture must be improved to incorporate Hund-rule-type correlations on the ions. The recent attempts in this direction by Liu[21] appear hopeful.

An important measurement which remains to be made on this system is to study whether the spin-wave excitations disappear into the energy gap induced by the antiferromagnetic interaction in the ordered state, and to study this as a function of temperature, as has been done for the cases of iron and nickel.[20,25-27] It should also be noted that if a Cr-Mn alloy was chosen so that its Fermi level was significantly different than its value in the present system, the spatial extent of the Bloch wave functions at the Fermi level would be different from those of the free atom. In this case one would then hope to see form factors which are quantitatively different from free-atom form factors. It would be interesting to choose such an alloy and repeat the present experiments for the spin-wave form factor as well.

ACKNOWLEDGMENTS

The authors wish to thank F. A. Schmidt for kindly supplying the crystals used in the present investigations. Thanks are also due to R. A. Reese for help with taking some of the data. The authors also wish to acknowledge helpful discussions with S. H. Liu, B. N. Harmon, and H. A. Mook. One of the authors (S. K. S.) wishes to acknowledge the hospitality of the Solid State Science Division at Oak Ridge National Laboratory for one phase of these experiments.

*Work performed for the U.S. ERDA under contract No. W-7405-eng-82.

†Present address: Solid State Div., Argonne National Laboratory, Argonne, Ill. 60439.

‡Present address: Institute for Materials Research, National Bureau of Standards, Washington, D.C. 20234.

§Operated by Union Carbide Corp. U.S. ERDA.

[1]A. W. Overhauser, Phys. Rev. Lett. 4, 462 (1960); Phys. Rev. 128, 1937 (1962).

[2](a) W. A. Lomer, Proc. Phys. Soc. Lond. 80, 489 (1962); (b) T. M. Rice and B. I. Halperin, Phys. Rev. B 1, 509 (1970).

[3]W. E. Evenson, G. S. Fleming, and S. H. Liu, Phys. Rev. 178, 930 (1969).

[4]R. P. Gupta and S. K. Sinha, Phys. Rev. B 3, 2401 (1971).

[5]C. Windsor, J. Phys. F 2, 742 (1972).

[6]R. M. Moon, W. C. Koehler, and A. L. Trego, J. Appl. Phys. 37, 1036 (1966).

[7]C. Stassis, G. R. Kline, and S. K. Sinha, Phys. Rev. Lett. 31, 1498 (1973); Phys. Rev. B 11, 2171 (1975).

[8]J. Als-Nielsen and O. W. Dietrich, Phys. Rev. Lett. 22, 290 (1969).

[9]S. K. Sinha, S. H. Liu, L. D. Muhlestein, and N. Wakabayashi, Phys. Rev. Lett. 23, 311 (1969).

[10]J. Als-Nielsen, J. D. Axe, and G. Shirane, J. Appl. Phys. 42, 1666 (1971).

[11]Y. Tsunoda, Y. Hamaguchi, and N. Kumitani, J. Phys. Soc. Jpn. 32, 394 (1972).

[12]F. A. Fedders and P. C. Martin, Phys. Rev. 143, 245 (1966).

[13]H. Yamada and M. Shimizu, J. Phys. Soc. Jpn. 22, 1404 (1967); 25, 1001 (1969).

[14]J. B. Sokoloff, Phys. Rev. 185, 770 (1969); 185, 783 (1969).

[15]S. H. Liu, Phys. Rev. B 2, 2664 (1970).

[16]Satya Pal, J. Chem. Phys. 60, 2741 (1974).

[17]M. J. Cooper and R. Nathans, Acta Crystallogr. 23, 357 (1967).

[18]N. J. Chesser and J. D. Axe, Acta Crystollogr. A 29, 160 (1973).

[19]A. J. Freeman and R. E. Watson, Acta Crystollogr. 14, 231 (1961).

[20]J. W. Lynn (unpublished).

[21]S. H. Liu (unpublished).

[22]R. G. Barnes and T. P. Graham, Phys. Rev. Lett. 8, 248 (1962); J. Appl. Phys. 36, 938 (1965).

[23]L. W. Bos and D. W. Lynch, Phys. Rev. B 2, 4567 (1970).

[24]K. H. Oh, B. N. Harmon, S. H. Liu, and S. K. Sinha, Phys. Rev. B (to be published).

[25]H. A. Mook and R. M. Nicklow, Phys. Rev. B 7, 336 (1973).

[26]H. A. Mook, R. M. Nicklow, E. D. Thompson, and M. K. Wilkinson, J. Appl. Phys. 40, 1450 (1969).

[27]H. A. Mook, J. W. Lynn, and A. M. Nicklow, Phys. Rev. Lett. 30, 556 (1973).